Exp Fluids (2011) 51:969–985
DOI 10.1007/s00348-011-1123-1

RESEARCH ARTICLE

A procedure based on proper orthogonal decomposition for time-frequency analysis of time series

Giacomo Valerio Iungo · Edoardo Lombardi

Received: 12 April 2010 / Revised: 11 April 2011 / Accepted: 4 May 2011 / Published online: 18 May 2011

Abstract A procedure for time-frequency analysis of time series is described, which is mainly inspired by singular-spectrum analysis, but it presents some modifications that allow checking the convergence of the results and extracting the detected spectral components through a more efficient technique, especially for real applications. This technique is adaptive, completely data dependent with no a priori assumption and applicable to non-stationary signals. The principal components are extracted from the signals and sorted by their fluctuating energy; moreover, the time variation of their amplitude and frequency is characterized. The technique is first assessed for multi-component computer-generated signals and then applied to experimental velocity signals. The latter are acquired in proximity of the wake generated from a triangular prism placed vertically on a plane, with a vertical edge against the incoming flow. From these experimental signals, three different spectral components, connected to the dynamics of different vorticity structures, are detected, and the time histories of their amplitudes and frequencies are characterized.

1 Introduction

Fluid dynamic signals are generally characterized by significant fluctuations that must be characterized in order to investigate on their physical origins. In several conditions, as for instance in wakes and jets, the flow fluctuations may show dominating spectral components, which can be singled out through the conventional Fourier transform. However, this technique gives only a time-invariant amplitude and frequency for each spectral component and thus becomes highly inappropriate for non-stationary signals. By considering for instance fixed-point measurements carried out in proximity of a wake, shedding of vorticity structures with different intensities and a varying distance from the measurement point can produce amplitude and/or frequency modulations in the acquired signal (AM–FM signal). Therefore, time analysis of the amplitude and frequency of the different spectral components is needed in order to investigate on the corresponding fluid dynamic phenomena.

For time-frequency analysis of AM–FM monocomponent time series, an evaluation of the time variation of the amplitude is represented by the so-called envelope of the signal, while regarding its spectral characteristics, the so-called instantaneous frequency (IF) is used. A benchmark of the most promising techniques to calculate the IF and envelope is reported in Huang et al. (2009), in which the most popular demodulation technique is considered to be the Hilbert transform (HT), see, e.g., Bendat and Piersol (1986). In case a multi-component signal is considered, the different AM–FM monocomponents must be singled out and separated before performing their demodulation. For instance, Sreenivasan (1985) carried out the monocomponent extraction through ad hoc band-pass filters; however, this technique is non-adaptive as it requires a filtering customization for each signal.

Alternatively, the wavelet transform may directly be applied to multi-component signals in order to characterize the time variation of all the spectral components present in a certain frequency range and instantaneously contributing to the signal fluctuations. Component extraction may also be performed by using, for instance, the so-called wavelet

G. V. Iungo (✉) · E. Lombardi
Department of Aerospace Engineering, University of Pisa,
via Caruso, 56126 Pisa, Italy
e-mail: valerio.iungo@epfl.ch

ridges, as reported in Carmona et al. (1998), or the technique proposed in Buresti et al. (2004), in which the main spectral components are detected qualitatively or statistically from the energy map calculated through the wavelet transform, and then each component is extracted through band-pass filtering also based on the wavelet transform. A more sophisticated wavelet decomposition is proposed by Olhede and Walden (2004), which enables spectral components to be extracted through ad hoc filter banks, but with band-edge imperfections in correspondence of the boundary of contiguous frequency sub-bands for components spanning at least two sub-bands, and by almost loosing the non-linear characteristics of the signal.

Another technique for component detection and extraction is the empirical mode decomposition (EMD) proposed by Huang et al. (1998), combined with the HT in the so-called Hilbert–Huang transform (HHT). EMD is an empirical technique producing a completely data-dependent (a posteriori) basis, in which its components, denoted as intrinsic mode functions (IMF), are not orthogonal, although several investigations have shown that the degree of non-orthogonality of the IMFs is very low. Nevertheless, the primary limitation of EMD is its fixed frequency resolution, which depends only on the sampling frequency and on the number of samples of the analyzed signal. In fact, EMD is basically a bank of dyadic filters, as proved, e.g., by Flandrin et al. (2004).

A technique based on the Karhunen–Loève expansion for decomposition of multicomponent time series is the singular-spectrum analysis (SSA). This technique requires the definition of the so-called window length or embedding dimension, N_{period}, which is the time length of the snapshots, which allows varying the frequency resolution of the time-frequency analysis. Since N_{period} is chosen, the eigen-decomposition of the lagged covariance matrix of the signal (see Broomhead and King 1986), which has a Toeplitz structure, is performed. SSA is found to be very useful for component detection and extraction from very short and noisy signals, see, e.g., Vautard et al. (1992), although the obtained principal components are characterized by a reduced dimension with respect to the source signal, i.e., a loss of $N_{\text{period}} - 1$ samples occurs. However, in Vautard et al. (1992), a method to obtain reconstructed components is presented in order to recover the original time length of the source signal. In Pastur et al. (2008), an interesting application of SSA for the analysis of the intermittency of two different spectral components present in the flow over an open cavity is reported.

In the present paper, a procedure for time-frequency analysis of time series is presented, which is based on the proper orthogonal decomposition (POD in the following) and can be considered as a modification of SSA. In fact, the POD modes are evaluated through the application of the classic POD to an ad hoc data set consisting of time portions of the source signal, each one composed of the same number of samples, instead of performing the eigen-decomposition of the lagged covariance matrix of the signal as for SSA. This modification allows varying number of the produced time portions of the signal in order to check the convergence of the obtained results. The POD produces an orthogonal basis whose elements are sorted by their energy. The POD modes corresponding to higher energy represent the most significant signal fluctuations, and their Fourier analysis already provides spectral information related to each POD mode. However, and more importantly, the AM–FM monocomponents associated with each POD mode can be obtained through a procedure based on the convolution of the source signal with the relevant POD mode, suitably manipulated. This procedure can lead to an increased efficiency of the spectral component extraction with respect to the classic SSA, especially in case of real applications.

The present paper is organized as follows: the POD procedure for time-frequency analysis of fluid dynamic time series and the technique for AM–FM monocomponent extraction are described in Sect. 2. In that section, the application of the POD procedure to different multi-component computer-generated signals is also reported. The technique is then applied to hot-wire anemometry signals acquired in proximity of the wake generated from a triangular prism (Sect. 3). Finally, some conclusions are drawn in Sect. 4.

2 POD procedure for time-frequency analysis of time series

2.1 Procedure and spectral component extraction

Proper orthogonal decomposition (POD) is a method providing an orthonormal basis for the modal decomposition of an ensemble of data functions. Therefore, a zero-mean random process $u(\mathbf{x}, t)$, where $\mathbf{x}$ is a space-vector $\mathbf{x} = x_1, \ldots, x_N$ and t is time, may be represented through a linear combination of deterministic functions, the POD modes, $\phi_j(\mathbf{x})$:

$$u(\mathbf{x}, t) = \sum_{j=1}^{M} \phi_j(\mathbf{x}) a_j(t) \tag{1}$$

where $\phi_j(\mathbf{x})$ are the eigen-functions of the covariance function of the analyzed process and represent the typical realizations of the process in a statistical sense, while $a_j(t)$ are uncorrelated coefficients denoted as principal components.

POD provides a modal decomposition that is completely a posteriori, data dependent and does not neglect the

non-linearities of the original dynamical system, even being a linear procedure; furthermore, the POD basis is orthogonal. The most peculiar feature of POD is optimality: among all linear decompositions it provides the most efficient detection, in a certain least squares optimal sense, of the dominant components and trends of an infinite-dimensional process.

Let us consider a generic zero-mean time series $u(t)$, which can represent a measurement performed in a fixed point of the flow field with a sampling frequency F_{samp} and a total number of samples equal to N_{samp}. If the signal $u(t)$ is a stationary process with infinite energy (i.e., it is not square-integrable since it does not vanish for t tending to infinite), POD modes are classic harmonic functions, as highlighted in Lumley (1970), and can be considered as generalized Fourier modes; nonetheless, an advantage in using POD is still present since the POD modes are sorted by their energetic significance. However, $u(t)$ may also be a non-stationary process and then the POD modes represent the most typical realizations of the process, sorted by their significance, and can be generic functions.

For SSA, the eigen-decomposition of the lagged covariance matrix of the signal is performed, whereas for the present procedure, the classic POD is used, and thus, a certain number of observations of the analyzed process are required, the so-called snapshots. To this end, time portions of the source signal $u(t)$ are generated, all with the same number of samples, N_{period}, denoted as embedding dimension. As well described in Vautard et al. (1992) for SSA, also for this procedure, a crucial task is represented by the choice of the embedding dimension, which is strictly related to the frequency resolution of the analysis; in other words, if Δf is the required frequency interval between two consecutive elements of the signal power spectrum, then N_{period} will be equal to the ratio between the sampling frequency and the frequency resolution, $F_{\text{samp}}/\Delta f$. Therefore, the higher is the embedding dimension, the higher is the frequency resolution of the spectral analysis. The typical approach for a time-frequency analysis consists in gradually increasing the embedding dimension, although it raises the computational cost of the procedure, in order to increase the frequency resolution and, thus, to attempt of capturing each spectral component of interest through different POD modes.

An adequately high number of snapshots are required to perform a satisfactory POD, i.e., in order to separate the typical realizations of the main phenomena from other random processes (see e.g., Buffoni et al. 2006). Generally, the number of snapshots, N_{snap}, is gradually increased through a sensitivity analysis, so that the convergence of the POD eigenvalues and of the most energetic POD modes is obtained, which is a very useful feature for real applications. In case a non-sufficient number of snapshots are produced from adjacent time portions of $u(t)$, a higher number of snapshots can be generated through partially overlapped time portions of the signal (for a given N_{period} and N_{snap} the right time lag must be evaluated in order to produce snapshots uniformly distributed along the time length of the signal). Obviously, this technique decreases the statistical independency of the process observations; however, this method turns out to be very useful to annihilate all random influences or disturbs present in a signal and better highlight all the typical realizations of the process.

Once the required number of samples for each snapshot, N_{period}, is chosen and the total number of snapshots, N_{snap}, is fixed, a matrix M is generated, whose rows are the time series of the snapshots; therefore, the size of M is $N_{\text{snap}} \times N_{\text{period}}$. Subsequently, the covariance matrix of M is evaluated as $C = M^T M$. C is a square matrix of size N_{period}, and each element C_{ij} represents the scalar product between the two respective columns of M, i.e., between the vectors composed of the values assumed by the samples with indexes i and j for the different snapshots. C is Hermitian symmetric and non-negative definite; thus, its eigenvalues are real and non-negative. The eigenvectors are orthogonal and are normalized through the L_2-norm so that the eigenvalues represent the energy associated with the respective eigenvectors. From a geometrical point of view, the eigenvectors represent the principal axes of C and are the so-called POD modes.

With reference to Eq. 1, by considering a time series $u(t)$, the space vector $\mathbf{x}$ becomes one-dimensional and represents the index of the samples of a certain snapshot ($x = 1, \ldots, N_{\text{period}}$), while the time, t, becomes the index of the snapshot ($t = 1, \ldots, N_{\text{snap}}$). Any snapshot, i.e., each row of the matrix M, is represented through a linear combination of the POD modes, $\phi(j)$:

$$M_i = \sum_{j=1}^{N_{\text{period}}} \phi(j) a_i(j) \tag{2}$$

where $a_i(j)$ are denoted as principal components, which are evaluated through the following projection:

$$a_i(j) = \langle M_i, \phi(j) \rangle \tag{3}$$

where $\langle \bullet, \bullet \rangle$ is the scalar product. Equation 2 proves the completeness and the uniqueness of the POD; moreover, the element of that series $\phi(j)a_i(j)$ represents the spectral contribution related to the POD mode $\phi(j)$ present in the snapshot M_i. If different eigenvectors are considered, their respective spectral components are characterized by a generic level of correlation, which is strictly related to their physical origins.

This procedure to evaluate the POD modes is used in case the number of samples of each snapshot, N_{period}, is lower than the total number of the snapshots, N_{snap}, which is the typical situation for this work, in which computer-generated and experimental signals are analyzed. Conversely, when N_{period} is higher than N_{snap}, which is the typical situation for data obtained from numerical simulations, the computational effort required to evaluate the eigen-functions of the covariance matrix, C, can be reduced with the method of snapshots or strobes proposed by Sirovich (1987). In this case, C is evaluated as $C = MM^T$, in order to reduce the dimension of the covariance matrix, so that C is a square matrix of size N_{snap} and each element C_{ij} represents the scalar product between the two respective rows of M, i.e., between the two respective snapshots. The consequent POD modes, ϕ_i, are expressed as a linear combination of the snapshots with the respective eigenvectors of C, b_i:

$$\phi_i = M^T b_i \tag{4}$$

Consequently, the POD modes are in number of N_{snap}, and the size of each one is N_{period}.

The first computer-generated signal used to assess the POD procedure for time-frequency analysis is a stationary time series composed of three different spectral components ($f_1 = 40$ Hz, $f_2 = 60$ Hz, and $f_3 = 70$ Hz) and white noise with an energy equal to 23% of the total energy of the signal:

$$y_1 = \sin(2\pi f_1 t) + 2\sin(2\pi f_2 t) + 4\sin(2\pi f_3 t) + WN \tag{5}$$

The signal is sampled with a frequency of 1 kHz.

The POD procedure for time-frequency analysis is applied by using for this test-case 10^4 snapshots (the convergence analysis of the POD will be discussed in the following), which represent adjacent time portions of the signal, each comprising 501 samples, i.e., the used frequency resolution is about 2 Hz, which enables to separate the different spectral contributions being lower than their minimum spectral separation. Being the number of snapshots, N_{snap}, higher than the number of the samples of each snapshot, N_{period}, the POD is performed in the classical manner, and the number of the POD modes is equal to $N_{\text{period}} = 501$. The eigenvalues reported in Fig. 1, which represent the fluctuating energy of the respective POD modes, are reported as percentage of the total energy of the signal and show that just the first six POD modes are characterized by a significant fluctuating energy, and thus, they are the only POD modes to be considered for the component extraction.

The Fourier power spectra of the first eight normalized POD modes are reported in Fig. 2. The most energetic POD modes, with the same energy, are POD modes 1 and 2, which are characterized by a dominant frequency of

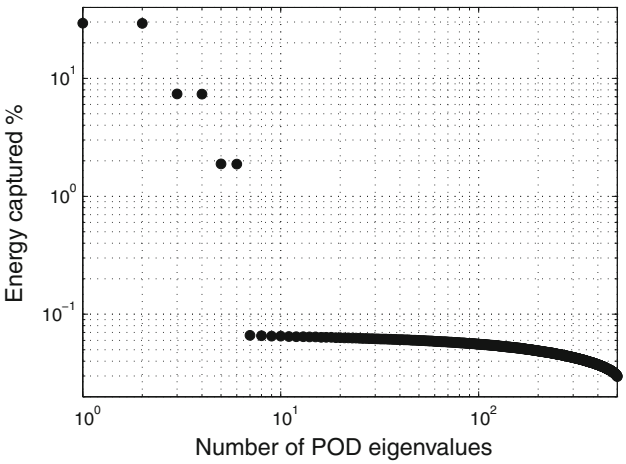

Fig. 1 POD eigenvalues evaluated for the computer-generated signal y_1

70 Hz, as expected being the most energetic spectral component of y_1 characterized by this frequency. From Fig. 2, it is seen that these two POD modes are characterized by the same power spectrum; however, from their respective time series (not reported for the sake of brevity), it is found that they are in quadrature, being elements of an orthogonal basis. This feature was expected because, as highlighted, e.g., in Vautard et al. (1992), a pair of eigen-elements with nearly equal energy is detected when a periodic dynamics is present in a signal.

The POD modes 3 and 4 are related to the component at frequency $f_2 = 60$ Hz, while 5 and 6 to the component at $f_1 = 40$ Hz; as expected, they are sorted by their energy. The remaining POD modes do not show any dominant spectral component and are due to white noise, but they are not analyzed because, as shown in Fig. 1, their relative energy is negligible.

As already mentioned, an advantage of this technique is the possibility of evaluating the convergence and stability of the eigen-elements obtained from the POD procedure with increasing number of snapshots, N_{snap}; in effect, the trend of the POD eigenvalues and of the Fourier power spectra of the most energetic POD modes can be checked. As shown in Fig. 3a, the POD eigenvalues reach asymptotic values for a number of snapshots higher than 100. Furthermore, by analyzing the Fourier power spectra of the POD mode 6 (Fig. 3b), i.e., the POD mode of interest with the lowest energy and, thus, easily affected by white noise, for $N_{\text{snap}} < 50$ this POD mode is basically a random function, whereas for a higher number of snapshots, the frequency of interests $f_1 = 40$ Hz appears, although influenced by the other spectral contributions. With increasing N_{snap}, the spectral component of interest is isolated, and the convergence of the POD mode is reached.

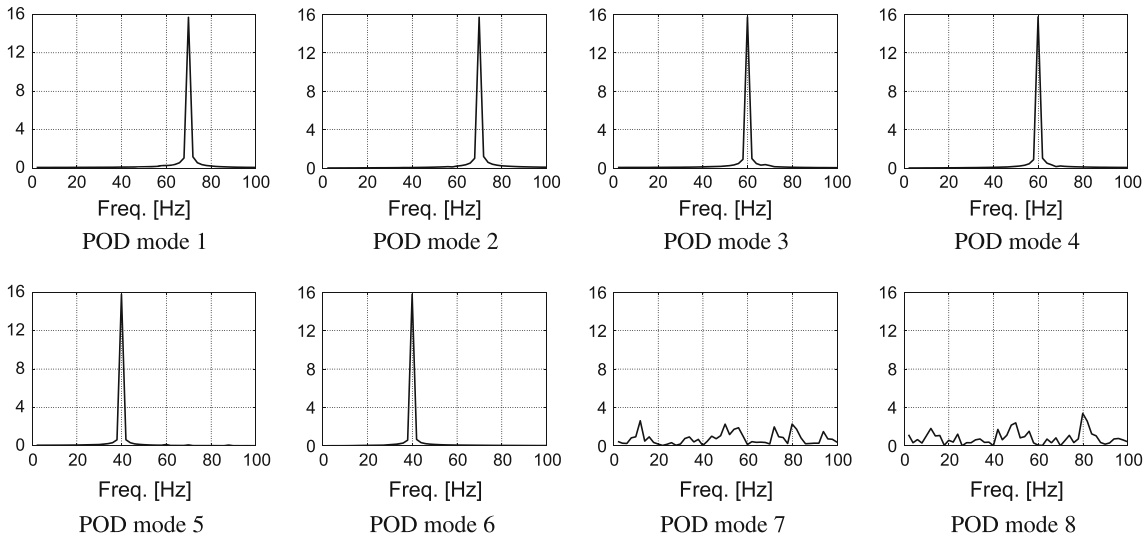

Fig. 2 Fourier power spectra of the first eight normalized POD modes evaluated for the signal y_1

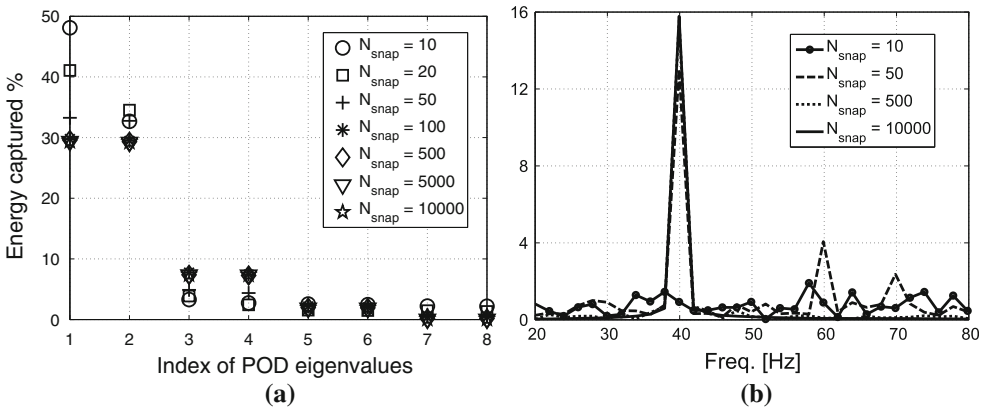

Fig. 3 Convergence of the POD procedure applied to y_1 by increasing the number of snapshots, N_{snap}: **a** first eight POD eigenvalues; **b** Fourier power spectrum of POD mode 6

From the power spectra of the POD modes, the dominant frequencies of the signal are detected and sorted by their energy; however, their contribution along the time length of the whole source signal is not determined yet. Then, the technique for AM–FM monocomponent extraction from a source signal is based on the convolution of the latter with the considered POD mode. However, a generic POD mode is not a symmetric filter, and thus, the convolution produces a certain phase shift, $\Delta\varphi$, on the extracted principal component with respect to the source signal. A phase-correction of the extracted principal component may be performed through the convolution of the source signal with the POD flip-mode, which is the reversed signal of the POD mode. However, a more robust procedure, and with lower computational effort, is based on performing a single convolution of the source signal with the POD conv-mode, a symmetric filter obtained from the convolution of a POD mode with its respective POD flip-mode.

An important step regarding principal component extraction through the convolution procedure consists in avoiding any amplification or damping. The basic idea of the filtering is that the convolution of a certain POD conv-mode with itself must produce the POD conv-mode without any amplification or damping. In order to reach this goal, the result of the convolution must be normalized through the norm of the convolution of the POD conv-mode with itself and then multiplied with the norm of the POD conv-mode in order to restore its initial energy. Therefore, the result of the convolution must be multiplied by the factor K:

$$K = \frac{|\text{conv} - \text{mode}|}{|\text{convolution}(\text{conv} - \text{mode}, \text{conv} - \text{mode})|} \tag{6}$$

where $|\bullet|$ represents the L_1-norm, i.e., the sum of absolute values of the elements, consistently with the precision adopted for the convolution algorithm (all the code was

implemented in *Matlab*® and the command *conv* is used for the convolution and the command *norm*(:,1) is used to calculate the L_1-norm).

As regards the computer-generated signal y_1, the three different spectral components are now extracted through the convolution of y_1 with the respective POD modes. The extracted spectral components are reported in Fig. 4 with their moduli obtained through the HT (calculated with *Matlab*® through the command *hilbert*). The HT enables to evaluate the quadrature of a time series, which is the imaginary part of a complex function denoted as analytic signal and whose real part is the considered time series. The IF of the signal is evaluated as follows:

$$\mathrm{IF} = \frac{F_{\mathrm{samp}}}{2\pi}\frac{\mathrm{d}\varphi}{\mathrm{d}t} = \frac{F_{\mathrm{samp}}}{2\pi}\frac{\mathrm{Re}\frac{\mathrm{dIm}}{\mathrm{dt}} - \mathrm{Im}\frac{\mathrm{dRe}}{\mathrm{dt}}}{\mathrm{Re}^2 + \mathrm{Im}^2} \tag{7}$$

where φ is the instantaneous phase of the analytic signal, and Re and Im are its real and imaginary parts, respectively. The time derivation of *Re* and *Im* is performed through a finite difference scheme of fourth order. The envelope of the signal is equal to the modulus of the analytic signal. However, the IF and the envelope have physical meaning if only certain necessary conditions are satisfied, that is, the signal must be monocomponent, zero-mean locally and symmetric (see, e.g., Huang et al. (2009) for more details).

Starting from the most energetic spectral component, i.e., the one related to the POD mode 1 with $f_3 = 70$ Hz, its amplitude is equal to 4 (Eq. 5) and through the spectral component extraction, its mean value is found to be 3.996 with a standard deviation of 0.087 (about 2% of the mean value), demonstrating that the spectral contribution of interest is completely captured by this spectral component. The instantaneous frequency of the spectral component is also evaluated through the HT, and a mean value of 69.915 Hz and a standard deviation of 0.013 (about 0.02% of the mean value) are found.

Since the spectral component related to the POD mode 1 is extracted, a residual signal can be evaluated by subtracting the extracted spectral component from the source signal y_1. If the spectral component related to the POD mode 2 is then extracted, it is found to correspond to a

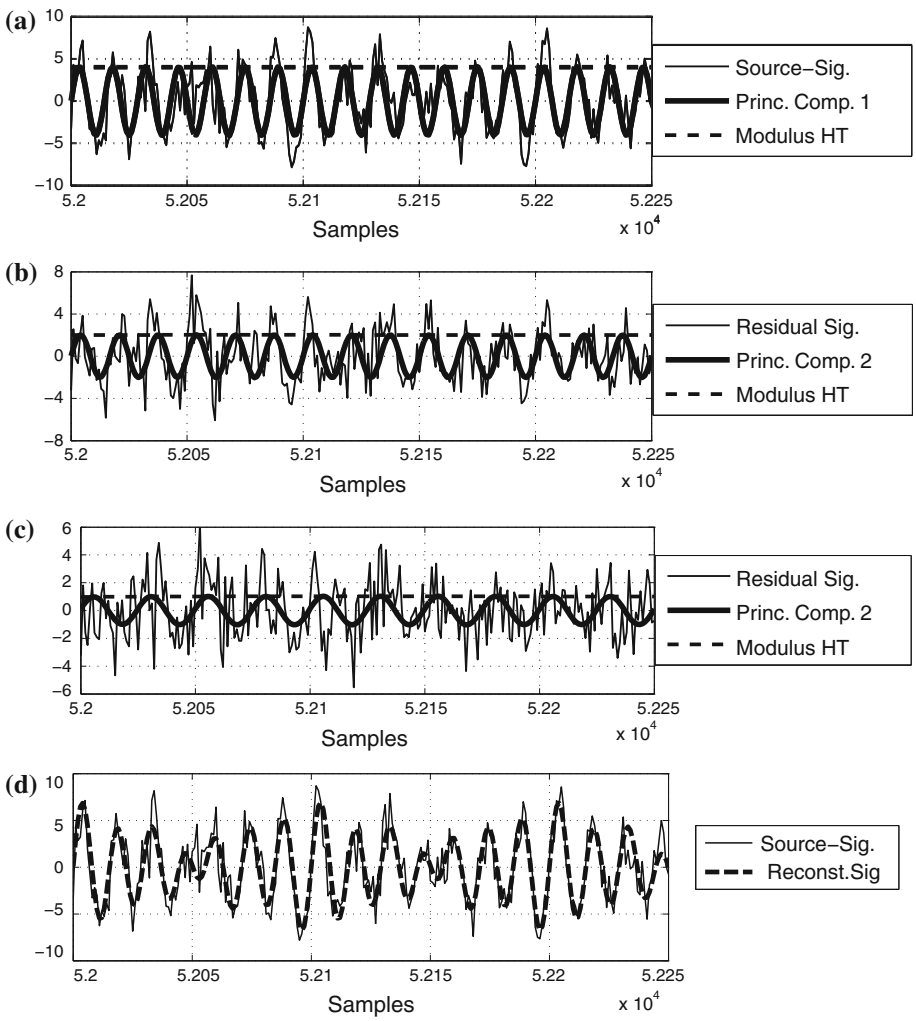

Fig. 4 Spectral components extracted from the source-signal y_1: **a** spectral component related to $f_3 = 70$ Hz; **b** spectral component related to $f_2 = 60$ Hz; **c** spectral component related to $f_1 = 40$ Hz; **d** reconstructed signal

practically null signal because POD mode 2 represents the same filter mask of the one related to POD mode 1. However, for real signals, a certain numerical error is present in proximity of the boundary of the spectral band, which is due to the discrete convolution performed in a finite time-frequency domain (see e.g. Iungo et al. 2009). Therefore, the spectral component of interest is mainly extracted by only using POD mode 1, and the one related to POD mode 2 is considered as a residue, which can be added to the one previously extracted. This is an important feature of the present technique with respect to other possible POD-based ones. For instance, in Vautard et al. (1992), a method to detect pairs of eigen-elements related to a periodic activity is proposed, and to completely extract each spectral component, both eigen-elements of the respective pair must be used.

Subsequently, the spectral component related to the POD mode 3 is extracted, i.e., the one corresponding to $f_2 = 60$ Hz. The time series of this spectral component is reported in Fig. 4b with its modulus evaluated through the HT (mean value of 2 and standard deviation of 0.087). From the HT of the extracted component, a mean value of the IF equal to 59.961 Hz is found, with a standard deviation equal to 0.025.

The last component related to the frequency $f_1 = 40$ Hz is extracted by using the POD conv-mode 5. The extracted component is reported in Fig. 4c (modulus with a mean value of 1.003 and standard deviation of 0.091). The mean IF evaluated through HT is equal to 39.995 Hz, with a standard deviation of 0.053.

Finally, by adding the three extracted spectral components together, it is seen in Fig. 4d that the reconstructed signal well reproduces the source signal y_1, except for the white noise, which is removed.

The test case of the computer-generated signal y_1 well highlights the advantages of the POD procedure for time-frequency analysis of time series: the only parameter to be chosen is the frequency resolution of the spectral analysis and thus the embedding dimension, N_{period}. This parameter can be gradually increased, although it raises the computational cost of the procedure to assess that possible spectral components are ascribed to different POD modes. Furthermore, this technique permits the convergence and stability of the POD eigen-elements to be checked, so that the number of snapshots produced from the source signal, N_{snap}, is gradually increased until the convergence of the POD eigen-elements is reached. Once the POD modes are calculated, the spectral components can be extracted in an automatic way starting from the most energetic one, calculating the residual signal and then extracting the following spectral components with less energy. The component extraction through the convolution method permits to capture a periodic activity of the signal by only using one POD mode of the pair with nearly equal energy characterizing it; therefore, no identification of pair of eigen-elements is required to completely reconstruct a spectral component. Finally, the characterization of the signal can be considered adequately performed when a certain percentage of the fluctuating energy of the source signal is extracted or when the dominant spectral contributions are captured.

2.2 Application of the POD procedure to computer-generated time series

Beside signals consisting of different spectral components, as simulated through the signal y_1, another case of interest in fluid dynamics is represented by a signal with a frequency modulation:

$$y_2 = \sin(2\pi f_1 t + A_2/f_2 \times \sin(2\pi f_2 t)) \tag{8}$$

where the carrier has a mean frequency $f_1 = 50$ Hz, and it is frequency modulated with an amplitude of $A_2 = 10$ Hz and a frequency $f_2 = 10$ Hz. The signal is sampled with a frequency $F_{\text{samp}} = 1$ kHz. The Fourier power spectrum of y_2, reported in Fig. 5, shows the typical result obtained from a Fourier analysis in the presence of a FM, i.e., the modulation of the carrier is represented through a set of spectral components that are symmetric with respect to the carrier frequency and have an appropriate energy cascade.

By considering the EMD, the signal y_2 is already an IMF being locally zero mean and symmetric; thus, it represents the only result of the EMD. By applying the wavelet transform, no further information is obtained in order to relate these symmetric contributions to a frequency modulation. However, the FM signal may be detected through an adaptive filtering with a central frequency equal to the one of the carrier and with increasing spectral amplitude.

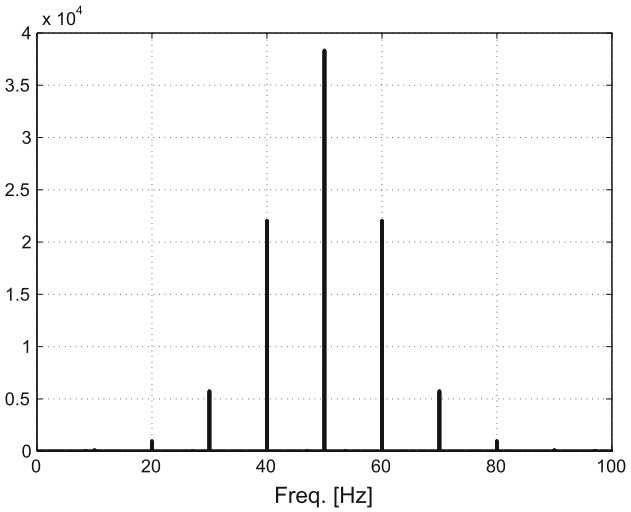

Fig. 5 Fourier power spectrum of the computer-generated signal y_2

The POD procedure is applied to y_2 with an extremely small embedding dimension equal to 5, i.e., with a very low-frequency resolution of 200 Hz ($F_{\text{samp}} = 1$ kHz), in order to attempt of capturing the contributions related to the FM in a single spectral component. From the signal, 5,000 snapshots are generated.

With the extraction of the spectral component related to the POD mode 1, the effectiveness of the POD procedure to detect FM signals is assessed. Indeed, the IF of this spectral component is perfectly the one of the signal y_2, that is, $f_1 + A_2\cos(2\pi f_2 t)$, with an error lower than 0.1%. However, a certain error is present in the evaluation of the component modulus; in fact, it is underestimated, and a fictitious AM is obtained with a frequency equal to the one of the FM, i.e., f_2, and a mean value of 0.83 with a standard deviation of 5%. A slightly better result is obtained by adding to this component the one related to the POD mode 2; in fact, the mean amplitude is increased to 0.88 with a standard deviation of 2%. This persisting error is due to the missed spectral components with higher frequency and smaller energy, which is a consequence of the poor frequency resolution used.

Better results are gained with the POD procedure by increasing the embedding dimension to 500, i.e., by using a higher-frequency resolution of 2 Hz. In fact, this increased embedding dimension allows detecting each symmetric component of the FM signal through different POD modes, being the spectral contributions at a distance of 10 Hz (see Fig. 5). Therefore, the first two POD modes are related to the frequency of the carrier f_1, while the remaining ones are grouped by 4 and correspond to the symmetric components with increasing frequency distance and decreasing energy. Therefore, the component extracted with only the POD mode 1 corresponds to the mean frequency f_1, and by adding further four POD modes, a FM contribution with increasing frequency and decreasing energy is added. The modulus and the IF of the extracted spectral components obtained by adding further POD modes, reported in Fig. 6, show that with only the POD mode 1, the carrier with constant frequency of f_1 and a constant underestimated modulus is obtained, whereas by adding further POD modes, a constant amplitude equal to one and the proper IF is obtained. Finally, the error on the evaluation of the modulus and of the IF is reported in Table 1 as a function of the number of the used POD modes. Though this technique seems to be sophisticated, in practice, it turns out to be rather straightforward. Furthermore, it may easily be rendered an automatic procedure thanks to POD optimality; in fact, components with decreasing energy are gradually added, and this permits to rapidly achieve the proper IF and to reduce the spurious AM typically found in the presence of FM.

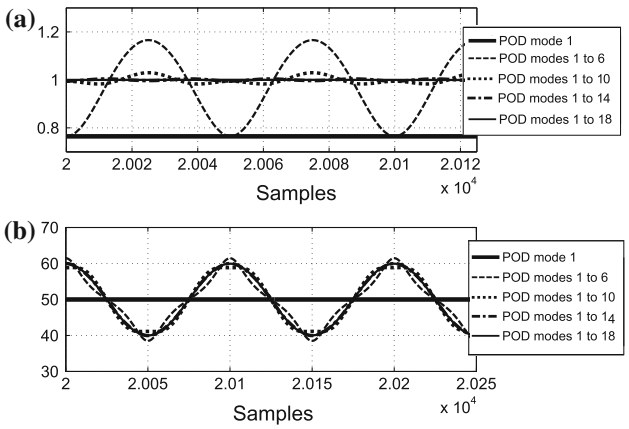

Fig. 6 Spectral components extracted from the signal y_2 by using a frequency resolution of 2 Hz and different POD modes: **a** modulus obtained through the HT; **b** IF calculated through the HT

Table 1 Error in the evaluation of the envelope and of the IF of the signal y_2 as a function of the number of the used POD modes. Frequency resolution set to 2 Hz

POD modes	Err. modulus (%)	Err. IF (%)
1	23.5	12.8
Up to 6	12.7	2.7
Up to 10	1.4	1.2
Up to 14	0.2	0.1
Up to 18	0.02	0.04

The next considered synthetic signal is the idealized Stokes wave in deep water, approximated at the second order:

$$y_3 = \frac{1}{2}a^2k + a\cos\omega t + \frac{1}{2}a^2k\cos 2\omega t \tag{9}$$

with $a = 1$, $ak = 0.2$, $\omega = 1/32$ and a sampling frequency $F_{\text{samp}} = 0.1$ Hz. The signal is plotted in Fig. 7a. The EMD produces only one IMF, reported in Fig. 7b, whose Hilbert spectrum (a 3D plot where the x-axis represents time, y-axis the frequency, and gray level the envelope of the extracted components) enables to detect the so-called intrawave modulation (Huang et al. 1998), that is, a variation of the amplitude and of the frequency for time lengths smaller than the period of the carrier (Fig. 7c).

In Huang et al. (1998), it is also assessed that this feature cannot be detected by using the wavelet transform and that the latter can only characterize interwave modulations. This is true, but an advantage of the wavelet transform with respect to EMD is represented by the possibility of adjusting the frequency resolution; in fact, by using a Morlet function defined as:

$$\psi(t) = \frac{1}{\sqrt{2\pi}}e^{j\omega_0 t}e^{-\frac{t^2}{2}} \tag{10}$$

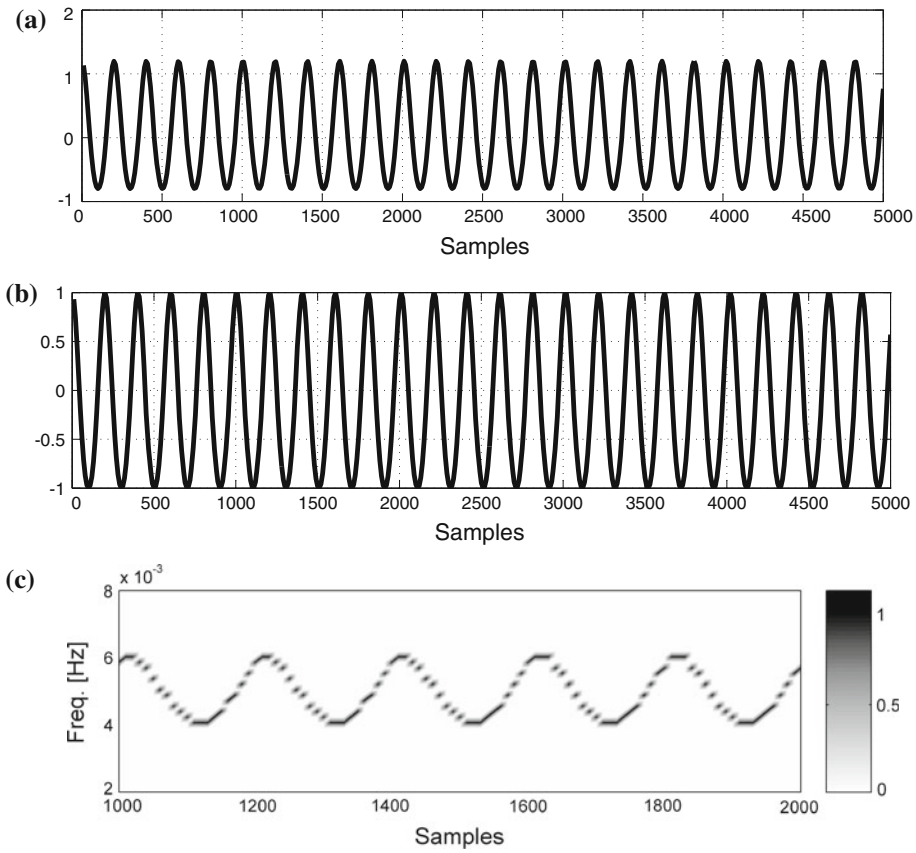

Fig. 7 EMD applied to the signal y_3: **a** signal; **b** IMF; **c** Hilbert spectrum

this can be performed by varying its central frequency. Thus, if a high-frequency resolution is used ($\omega_0 = 6\pi$), the two spectral components of the signal are clearly separated (Fig. 8a), whereas with a high time resolution ($\omega_0 = 2\pi$) just one main energy band is found (Fig. 8b).

By applying the POD procedure to the signal y_3 with an embedding dimension of 100, i.e., with a frequency resolution of 0.001 Hz, which enables to separate the two spectral components of the signal, four POD modes with a significant energy are found: The first couple is related to the component with a frequency equal to ω and the second one to the component with frequency equal to 2ω. The resulting Hilbert spectrum, reported in Fig. 9a, shows the two distinct spectral components with constant amplitudes, analogously to the result obtained through the wavelet transform with a high-frequency resolution shown in Fig. 8a. On the other hand, if the smaller embedding dimension of 20 is used, which corresponds to a frequency resolution of 0.005 Hz, the two components cannot be separated anymore and they are both simultaneously detected by the first four POD modes; the consequent Hilbert spectrum is reported in Fig. 9b, which is the same one obtained with the EMD. Concluding, this test case assesses once again the advantage of the POD procedure to adjust the time-frequency resolution, by varying the embedding dimension, in order to find the best result for a time-frequency analysis.

3 Application of the POD procedure to experimental fluid dynamic signals

The procedure based on the POD for component detection and extraction from time series is now applied to the case of hot-wire anemometry signals acquired in proximity of the wake generated from a triangular prism.

An experimental investigation on the near-wake flow field generated from a prism with equilateral triangular cross-section, aspect ratio $h/w = 3$, where h is the height and w the base edge of the model, and orientated with its apex edge against the incoming wind, was presented in Buresti and Iungo (2010). A sketch of the experimental setup is reported in Fig. 10, where the used frame of reference is also reported. The tests were carried out at a Reynolds number, based on w, of 1.5×10^5.

For this configuration, flow fluctuations at three prevailing frequencies were singled out, with different relative intensities depending on the wake regions. In particular, the frequency connected with alternate vortex shedding from the vertical edges of the prism was found to dominate in the

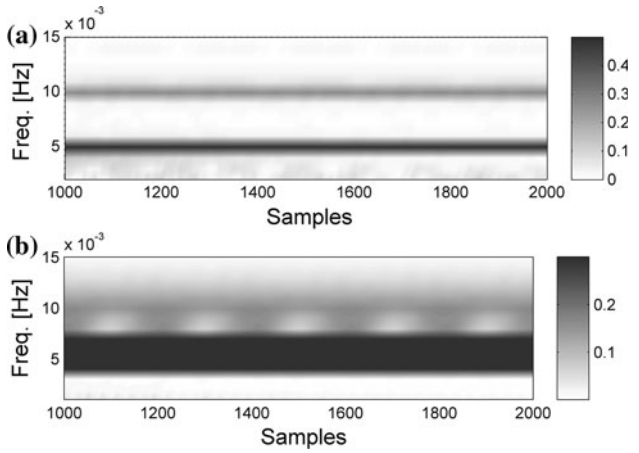

Fig. 8 Wavelet transform applied to the signal y_3: **a** central frequency $\omega_0 = 6\pi$; **b** central frequency $\omega_0 = 2\pi$

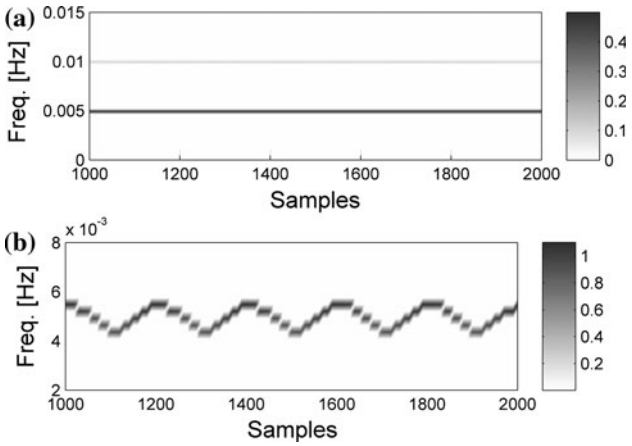

Fig. 9 Hilbert spectrum obtained from the POD procedure applied to the signal y_3: **a** high frequency resolution; **b** low-frequency resolution

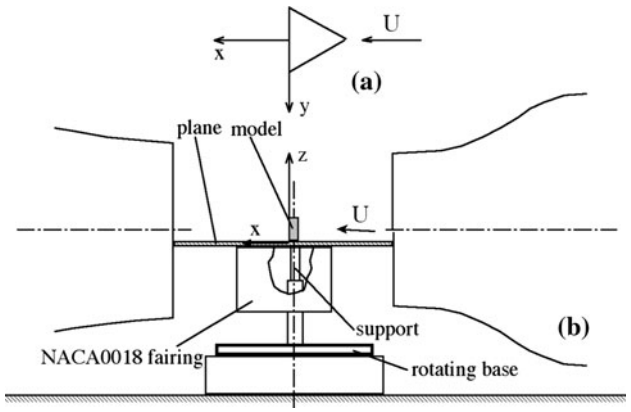

Fig. 10 Sketch of the experimental setup: **a** model orientation; **b** test layout

regions just outside the lateral boundary of the wake at a Strouhal number of about $\mathrm{St} = fw/U_\infty \approx 0.16$, where U_∞ is the freestream velocity. On the other hand, a lower frequency, at $\mathrm{St} \cong 0.05$, was found to prevail in the velocity fluctuations on the whole upper wake. Simultaneous measurements carried out over the wake of the prism at symmetrical locations with respect to the symmetry plane showed that these fluctuations correspond to a vertical, in-phase, oscillation of two counter-rotating axial vortices detaching from the front edges of the free-end. This finding was confirmed by the results of a LES simulation of the same flow configuration, described in Camarri et al. (2006), which also highlighted the complex topology of the upper near-wake produced by the vorticity sheets shed from all the edges of the prism. In Buresti and Iungo (2010), wake velocity fluctuations were also observed at an intermediate frequency $\mathrm{St} \cong 0.09$ and were found to prevail in the symmetry plane. By using the evidence provided by the above-mentioned LES simulation, by flow visualizations and by pressure measurements over the prism surface, it was suggested that they may be caused by a flag-like oscillation of the sheet of transversal vorticity shed from the rear edge of the body free-end, and approximately lying along the downstream boundary of the recirculation region in the central part of the near wake. The three above-described frequencies may also be found together for signals acquired aside the wake. Therefore, even if the fluctuations at the various frequencies are produced by the dynamics of different vorticity structures, they all contribute to the global oscillation of the wake.

We consider a velocity signal characterized by the presence of a single dominant spectral component, for instance the one connected to alternate vortex shedding at $\mathrm{St} \approx 0.16$. This is the case of the signal acquired aside the wake in correspondence to the point $x/w = 4$, $y/w = 1.5$, $z/h = 0.3$. The power spectrum of this signal evaluated through the Welch's method is reported in Fig. 11a. These velocity signals are acquired with a sampling frequency of 2 kHz, and they consist of 2^{16} samples.

Consecutively, to the detection of a dominant frequency for the considered signal, a first attempt to carry out a time-frequency analysis consists in applying the wavelet transform by using a Morlet function with a central frequency $\omega_0 = 6\pi$, in order to enhance its frequency resolution. The modulus of the wavelet coefficients, reported in Fig. 11c, confirms the presence of a dominant spectral component in proximity of $\mathrm{St} \approx 0.16$ and also enables to highlight its strong irregularity both in amplitude and frequency. The deriving wavelet spectrum is reported in Fig. 11b.

Let us now apply the POD procedure. From the power spectrum of the considered signal, only one dominant spectral component has been observed, and thus, a high-frequency resolution is not required for its time-frequency analysis. Consequently, the POD procedure is first applied with an embedding dimension of 101, which provides a high time resolution, i.e., by using a frequency resolution

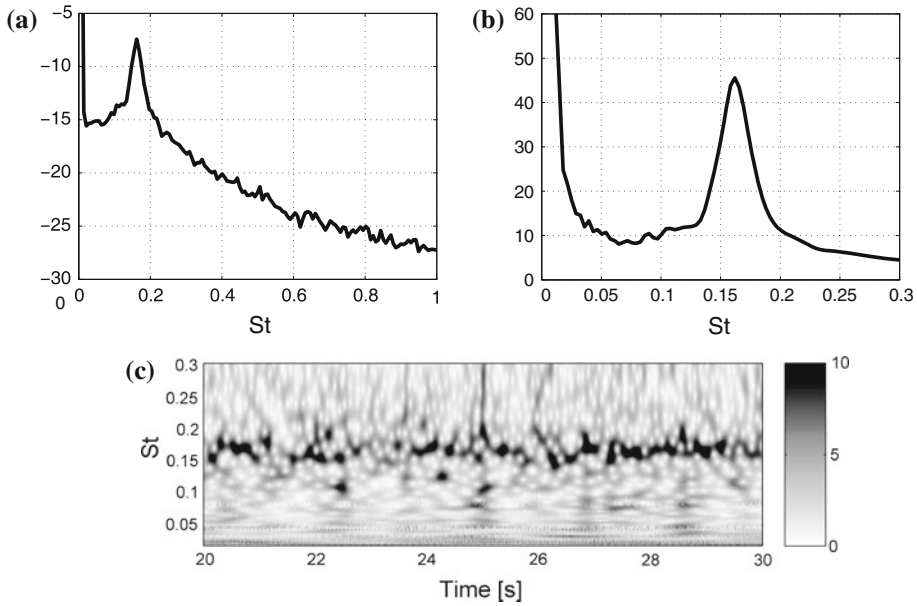

Fig. 11 Signal acquired at $x/w = 4$, $y/w = 1.5$, $z/h = 0.3$: **a** power spectrum; **b** wavelet spectrum; **c** map of the modulus of the wavelet coefficients

of about 20 Hz. An advantage of the POD procedure consists in the possibility of checking the stability and the convergence of the eigen-elements by gradually increasing the number of the produced snapshots; in effect, in Fig. 12, it is shown that for a number of snapshots higher than 10^3, the convergence of the POD eigenvalues is reached. For this analysis, 10^4 snapshots are used, which is a sufficiently high number to ensure the convergence of the POD eigenvalues, but still requiring a small time for the calculation. The SSA is also applied for this signal, and the respective eigenvalues, also reported in Fig. 12, are roughly the same ones obtained through the POD procedure.

The POD eigenvalues, which represent the energy associated with the respective POD modes, obtained through the POD technique are reported in Fig. 13a as percentage of the total energy of the source signal. The cumulative energy in Fig. 13b, i.e., the energy extracted by using a certain number of POD modes, shows that with only the first pair of POD modes roughly, the 35% of the fluctuating energy of the signal is captured, and with the first four POD modes the 50%, confirming the optimality of the POD to easily detect the core of the fluctuations of a signal without investigating on the remaining part.

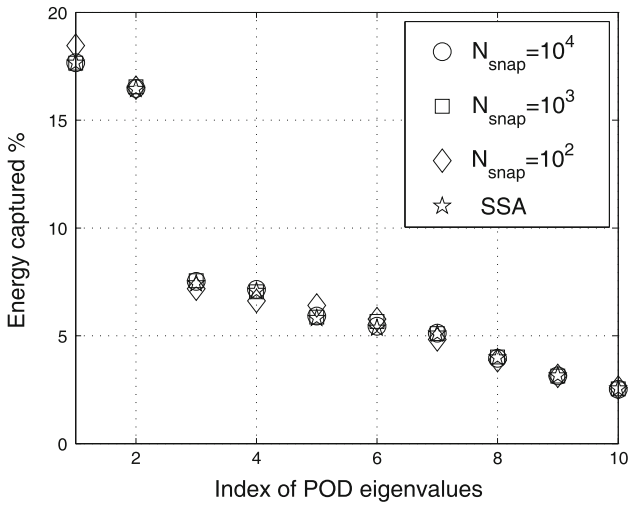

Fig. 12 POD eigenvalues evaluated for the signal acquired at $x/w = 4$, $y/w = 1.5$, $z/h = 0.3$ by varying the number of snapshots

From Fig. 13a, the first and second POD eigenvalues are found with a nearly equal energy, and thus, as already mentioned in Sect. 2, they are related to a periodic activity. In fact, by analyzing in Fig. 14 the time histories of the first two POD modes, they are found to be in quadrature and represent an oscillation with a frequency of about St $\approx$ 0.167, while the third and fourth POD eigenvalues are also coupled and their respective POD modes represent clearly a signal composed of two frequencies (about St $\approx$ 0.108 and St $\approx$ 0.216), i.e., AM and/or FM of a carrier at St $\approx$ 0.16. The modes obtained through SSA are exactly the same than the ones obtained through the POD technique.

Subsequently, the spectral component extraction is performed; indeed, in Fig. 15a, the Fourier power spectrum related to the component extracted through the POD mode 1 is shown, and from the one of the residual signal (Fig. 15b), i.e., the original signal from which the extracted component is subtracted, it is seen that it represents the main part of the dominant spectral component.

The Hilbert spectrum of the extracted component in Fig. 16 shows that this spectral component consists of the carrier at St $\approx$ 0.16 with AM–FM smaller then 10 Hz,

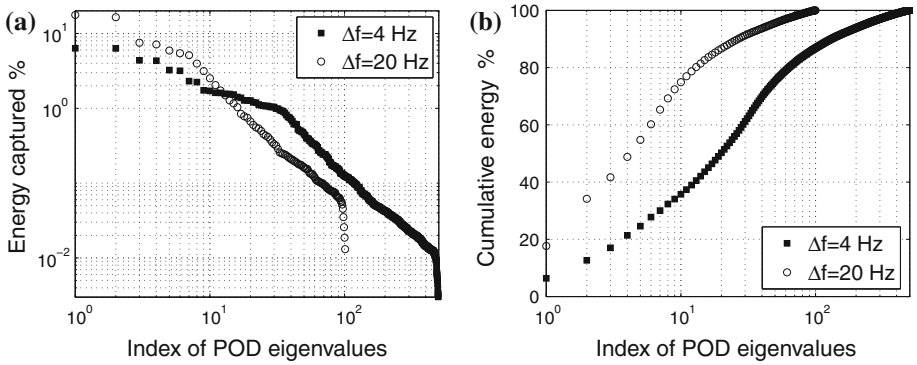

Fig. 13 POD eigenvalues evaluated for the signal acquired at $x/w = 4$, $y/w = 1.5$, $z/h = 0.3$: **a** eigenvalues as percentage of the total energy; **b** cumulative energy as percentage of the total energy

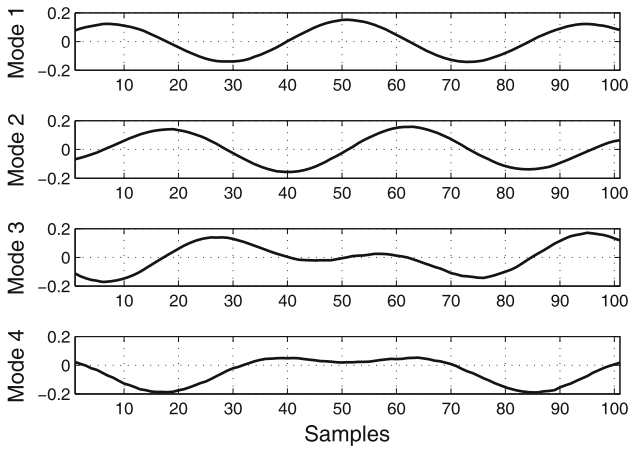

Fig. 14 Time series of the first four POD modes evaluated for the signal acquired at $x/w = 4$, $y/w = 1.5$, $z/h = 0.3$ with a frequency resolution of 20 Hz

consistently with the adopted frequency resolution of 20 Hz. The mean value of its IF is St = 0.162, and its standard deviation is 0.035. Regarding the envelope, the modulus of this component is characterized by a mean value of 1.542 and standard deviation of 0.647.

The component related to the POD mode 2 represents a residue of the component extracted through the POD mode 1, due to numerical errors made through the discrete convolution over a finite time-frequency domain, as explained in Sect. 2. More interesting is the evaluation of the contribution due to the POD mode 3, which represents AM–FM with frequency lower than 20 Hz, as shown with its power spectrum reported in Fig. 15c. The power spectrum of the residual signal obtained after the extraction of the first three POD modes is reported in Fig. 15d. The spectral component obtained from the first three POD modes has the following characteristics: IF mean St = 0.162, IF

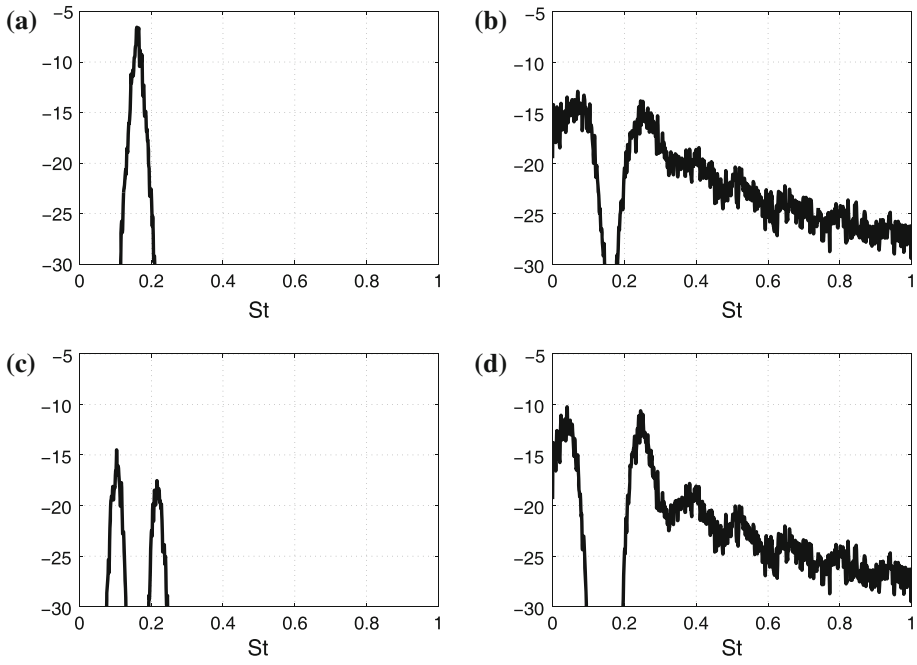

Fig. 15 Component extraction from the signal acquired at $x/w = 4$, $y/w = 1.5$, $z/h = 0.3$ by using a frequency resolution of 20 Hz. Fourier power spectra: **a** component with POD mode 1; **b** residual signal consequent to the extraction of the component related to the POD mode 1; **c** component with POD mode 3; **d** residual signal consequent to the extraction of the components related to the POD modes 1, 2 and 3

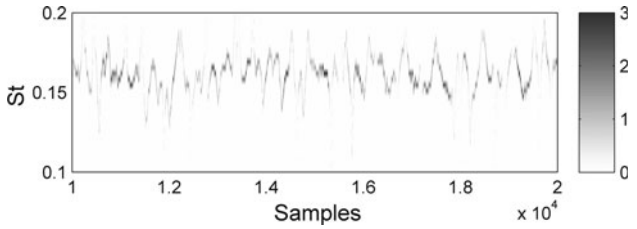

Fig. 16 Hilbert spectrum of the component extracted from the signal acquired at $x/w = 4$, $y/w = 1.5$, $z/h = 0.3$ by using a frequency resolution of 20 Hz and by using the POD mode 1

standard deviation 0.06, mean modulus 1.975, modulus standard deviation 0.897.

If the component extraction is now carried out through the SSA, with the method proposed in Vautard et al. (1992), by using the mode 1, the main spectral component is only partially extracted, as shown in Fig. 17a; however, when the extraction is performed by using the modes 1 and 2, the spectral component is completely captured (Fig. 17b). The spectral component obtained from the modes 1 and 2 has the following characteristics, which are practically the same obtained through the POD procedure by only using the POD mode 1: IF mean St = 0.162, IF standard deviation 0.038, mean modulus 1.555, modulus standard deviation 0.652. Summarizing, the POD technique permits to extract a spectral component by only using one POD mode of the pair associated with the periodic dynamics; conversely, SSA requires always the detection of pairs of eigen-elements that for multicomponent and very noisy signals may be a difficult task.

An analysis of the rate of presence of the extracted spectral component is also performed, inspired by the time-frequency analysis reported in Pastur et al. (2008); it is evaluated as the ratio between the number of samples for which the modulus of the component is higher than its mean value and the total number of samples of the source signal. Moreover, the time length of each occurrence is also evaluated, that is, the presence of this spectral component is about 50% of the total time length of the signal (0.501, 0.494, and 0.483 for the components extracted by using the POD mode 1, POD modes 1 and 2, POD modes 1, 2, and 3, respectively), and the mean time length of each occurrence is about 0.08 s (166 samples) if the only POD mode 1 is considered, whereas it is slightly reduced if the component due to the POD mode 2 is also considered (152 samples). When the component obtained from the first three POD modes is extracted, the mean time length of the occurrences is reduced to 72 samples; this is due to the further AM–FM added with the increasing number of considered POD modes.

Consecutively, an analysis with an increased embedding dimension of 501, i.e., with a frequency resolution of 4 Hz is performed, and by using the same number of snapshots of 10^4. This is the typical procedure used for real applications, indeed if different spectral components have been captured by a single POD mode, they could be separated by using an increased embedding dimension.

The evaluated POD eigenvalues are reported in Fig. 13a and the cumulative energy in Fig. 13b. With the first pair of POD modes, just the 13% of the total energy is captured in this case. Furthermore, it is shown that to reach the energy captured by the first pair of POD modes obtained by using the frequency resolution of 20 Hz, i.e., 35% of the total energy of the signal, in this case, about 10 POD modes must be selected.

The statistics related to the extracted spectral components, reported in Table 2, show that by considering further pairs of POD modes, the modulus of the component increases, as expected because more energy is added to the extracted signal, but also its fluctuation increases due to the added AM. For the same reason, the mean lifetime of the spectral component, mean Δ, decreases by considering further POD modes. However, the presence of the component along the whole time length of the signal, η, is practically unchanged by varying the number of selected POD modes, i.e., about 50% of total time length of the source signal. Regarding the IF, its mean value is practically unaffected, whereas its standard deviation increases due to the added FM represented by the further POD modes.

As mentioned above, to capture 35% of the total energy of the signal, 10 POD modes must be selected if a

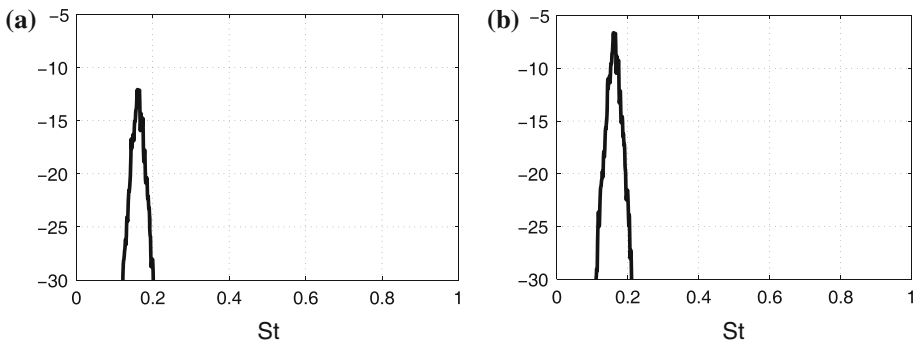

Fig. 17 Component extraction from the signal acquired at $x/w = 4$, $y/w = 1.5$, $z/h = 0.3$ through SSA. Fourier power spectra: **a** component with mode 1; **b** component with modes 1 and 2

Table 2 Statistics of the spectral component extracted from the signal acquired at $x/w = 4$, $y/w = 1.5$, $z/h = 0.3$ by using a frequency resolution of 4 Hz and a different number of POD modes

Num. POD modes	Mean mod.	σ mod.	Mean IF	σ IF	η	Mean Δ (samples)
2	1.08	0.49	0.162	0.022	0.49	502
4	1.24	0.54	0.162	0.022	0.50	267
6	1.35	0.58	0.161	0.025	0.49	194
8	1.49	0.63	0.163	0.035	0.49	173
10	1.56	0.65	0.162	0.036	0.49	162

frequency resolution of 4 Hz is used, whereas with a frequency resolution of 20 Hz, the same energy is captured by only the first 2 POD modes. By comparing these two spectral components evaluated by using different frequency resolutions and characterized by the same energy, it is seen that practically, their statistics are almost equal; indeed, roughly the same envelope is obtained for both used frequency resolutions, as can be seen from a time portion of the modulus of the components in Fig. 18a. However, the comparison of the IF in Fig. 18b highlights that although the statistics of the IF are almost equal for both cases, a slightly smoother IF is generally observed for the one obtained with the frequency resolution of 4 Hz, which is most probably a consequence of the reduced time resolution.

The time-frequency analysis of the hot-wire signal acquired at $x/w = 4$, $y/w = 1$ and $z/h = 0.9$ is also performed. The power spectrum of this signal evaluated through the Welch's method is reported in Fig. 19a. The map of the modulus of the wavelet coefficients, calculated through a Morlet function with $\omega_0 = 6\pi$ (Fig. 19c), shows that a large amount of the energy of this signal is included in a frequency range between St $\approx$ 0.03 and St $\approx$ 0.2; several spectral components seem to be present, but their detection is not sufficiently clear due to their comparable energy and limited spectral separation. However, the wavelet spectrum in Fig. 19b highlights the presence of three dominant spectral contributions at St $\approx$ 0.05, St $\approx$ 0.09, and St $\approx$ 0.16. As observed from the wavelet map, the extraction of these components through band-pass filtering is very challenging because they are highly modulated and spectrally close.

Before performing the spectral decomposition, the signal is filtered through a high-pass filter with a cutoff frequency of St = 0.03, in order to remove the typical low-frequency flow fluctuations that were known to be present in the wind tunnel freestream and, thus, avoiding to analyze spectral components with no physical meaning. However, if the high-pass filtering is not performed, the first pair of eigen-elements is related to these low frequencies, and the following ones are the components reported in the present analysis. The POD procedure is applied to the signal by using an embedding dimension of 1001, i.e., a frequency resolution of about 2 Hz, which can allow to associate the three spectral components to different POD modes. A total number of snapshots equal to 10^4 are produced. The obtained first 50 POD eigenvalues are reported in Fig. 20.

Starting with the extraction of the spectral contribution related to the most energetic POD mode, viz., POD mode 1, it is seen from its Fourier power spectrum, reported in Fig. 21, that it represents a narrow-band signal at St $\approx$ 0.05. As suggested in Buresti and Iungo (2010), this

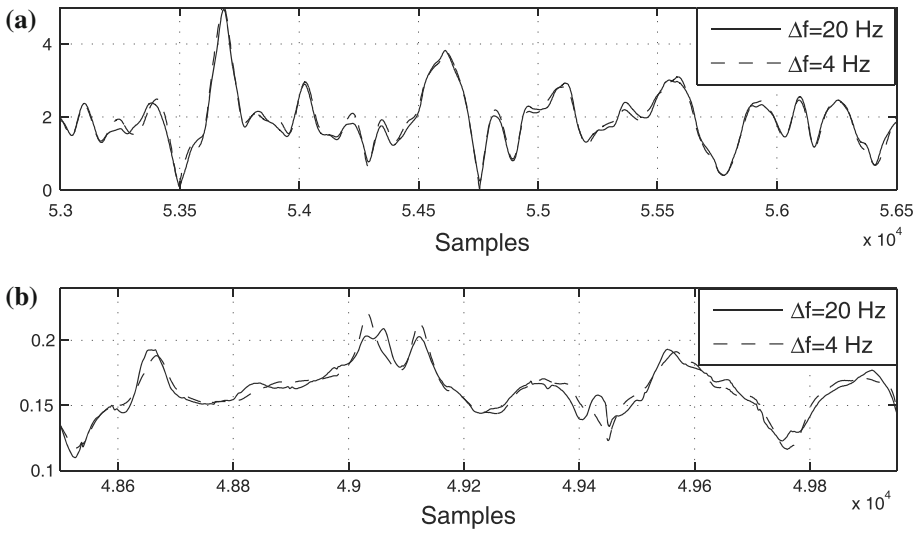

Fig. 18 Spectral components representing 35% of the energy of the signal acquired at $x/w = 4$, $y/w = 1.5$, $z/h = 0.3$ by using different frequency resolutions: **a** envelope; **b** IF

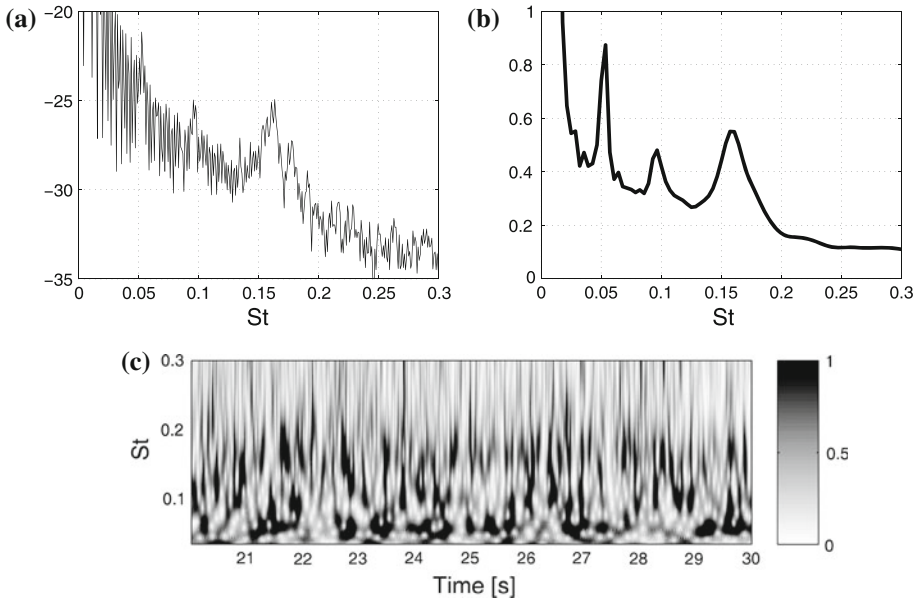

Fig. 19 Signal acquired at $x/w = 4$, $y/w = 1$, $z/h = 0.9$: **a** power spectrum; **b** wavelet spectrum; **c** map of the modulus of the wavelet coefficients

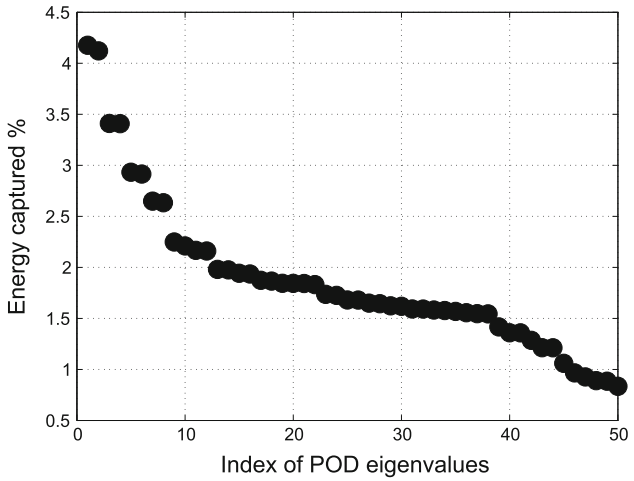

Fig. 20 First 50 POD eigenvalues evaluated for the hot-wire anemometry signal acquired at $x/w = 4$, $y/w = 1$, $z/h = 0.9$

spectral contribution is connected to the dynamics of a couple of axial vortices detaching over the model free-end. In effect, as this velocity signal was acquired at a relative high position, this phenomenon turns out to be the most energetic one.

The POD mode 2 is the one coupled to the POD mode 1, i.e., characterized by roughly the same power spectrum but with a phase shift of 90°. The spectral contribution extracted with the POD mode 2 from the residual signal, obtained after the extraction of the contribution due to the POD mode 1, represents a residue of the contribution previously extracted with the POD mode 1, due to numerical errors made through the discrete convolution over a finite time-frequency domain. In fact, this spectral component consists only of frequencies located in proximity of the boundary of the respective spectral band.

Moving to the extraction of the spectral contribution connected to the POD mode 3, the corresponding power spectrum shows that it is clearly due to the alternate vortex shedding, being characterized by a mean Strouhal number of St $\approx$ 0.16, while POD mode 4 is its coupled one.

The following analyzed POD mode, POD mode 5, represents a further contribution to the spectral component due to alternate vortex shedding, i.e., its AM and/or FM, being characterized by a mean IF of St $\approx$ 0.16. The POD mode 6 is its coupled one.

Interestingly, the spectral contribution related to the POD mode 7 is characterized by St $\approx$ 0.09, indicating that it is connected to the oscillations of the shear layer bounding the recirculation area located just behind the model. POD mode 8 is its coupled one.

Subsequently, the extracted spectral contributions are grouped by their mean IF in order to obtain AM–FM monocomponents. Therefore, the first monocomponent is obtained by adding the contributions due to the POD mode 1 and 2, the second with the POD modes from 3 to 6, and the last one with the POD modes 7 and 8. The statistics of these three spectral components, reported in Table 3, highlight that their rate of presence is almost the same, but the life time of the component at St $\approx$ 0.16 is almost half than the one of the remaining spectral components; this is due to the fact that by using only 8 POD modes, i.e., by extracting about 26% of the total energy of the signal, significant AM–FM of this component is considered through the POD modes 5 and 6. This feature is also confirmed by the higher standard deviation of the IF of this component.

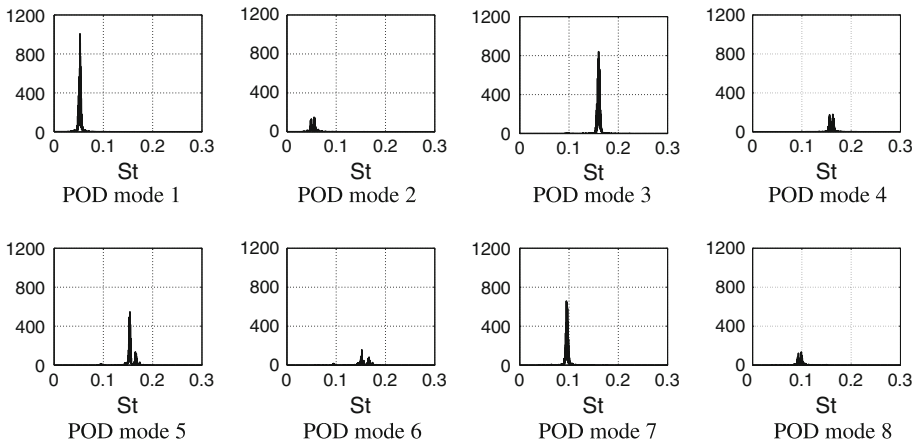

Fig. 21 Fourier power spectra of the components extracted with different POD modes for the signal acquired at $x/w = 4,\ y/w = 1,\ z/h = 0.9$

Table 3 Statistics of the spectral components extracted from the signal acquired at $x/w = 4,\ y/w = 1,\ z/h = 0.9$

POD modes used	Mean modulus	σ modulus	Mean IF	σ IF	η	Mean Δ (samples)
1, 2	0.09	0.05	0.052	0.004	0.43	1,177
3, 4, 5, 6	0.11	0.06	0.159	0.008	0.47	489
7, 8	0.07	0.03	0.096	0.006	0.48	1,051

In Fig. 22, the resulting Hilbert spectrum related to these three AM–FM monocomponents is reported, which permits to represent simultaneously the three AM–FM monocomponents. Furthermore, the three components are found to be practically uncorrelated, as can be seen from Fig. 23. Indeed, the correlation coefficient between the envelope of the component at St $\approx$ 0.05 and the one at St $\approx$ 0.16 is $e_{12} = -0.05$, the one between the component at St $\approx$ 0.05 and the one at St $\approx$ 0.09 is $e_{13} = 0.01$, and the remaining one $e_{23} = 0.01$. Therefore, this can assess that the physical origin of these flow fluctuations is due to the dynamics of different vorticity structures. Finally, in Fig. 24, the reconstructed signal obtained by adding the three AM–FM monocomponents is compared to the source signal, showing that this simplified signal represents the skeleton of the source signal from which the effects due to turbulence or to instrument noise are removed.

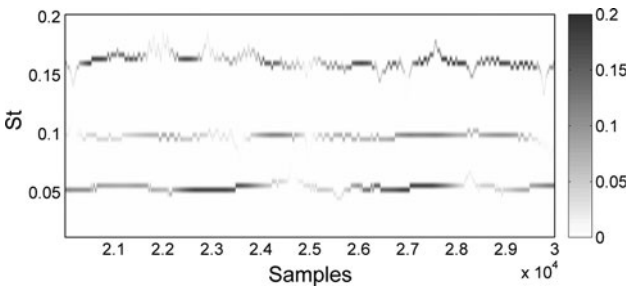

Fig. 22 Hilbert spectrum of the signal acquired at $x/w = 4,\ y/w = 1,\ z/h = 0.9$

4 Discussion and conclusions

A procedure based on the proper orthogonal decomposition (POD) for detection and extraction of components present in time series has been presented, which can be considered as a modification of singular-spectrum analysis. The proposed technique allows checking the convergence of the obtained results by varying the number of observations of the signal.

Each spectral component is extracted by only using one POD mode of the respective pair; this feature makes the technique more efficient especially for real applications. Consequently, methods for detection of POD mode pairs, which are typical for POD-based techniques, are not required.

Due to the POD optimality, an automated procedure for principal component extraction is used, and the fluctuations of a signal can be considered as adequately characterized when a certain fluctuating energy is extracted or when the main spectral components are captured. Furthermore, the extracted components can be grouped as a function of their mean frequency in order to produce amplitude-frequency-modulated monocomponents, which can be properly demodulated.

The procedure for component detection and extraction has been first assessed for computer-generated signals and then applied to hot-wire signals acquired in proximity of the wake generated from a triangular prism placed with a vertical edge against the incoming flow. From the

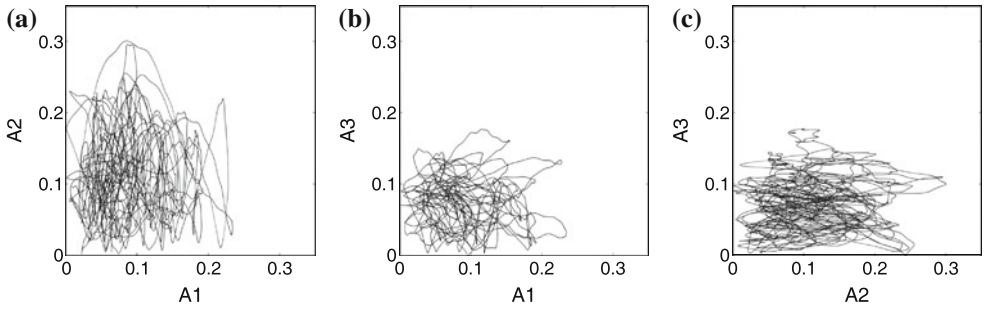

Fig. 23 Amplitudes of the components extracted from the signal acquired at $x/w = 4$, $y/w = 1$, $z/h = 0.9$. A_1 amplitude related to the component with St ≈ 0.05, A_2 amplitude related to the component with St ≈ 0.16, A_3 amplitude related to the component with St ≈ 0.09: **a** A_1 versus A_2; **b** A_1 versus A_3; **c** A_2 versus A_3

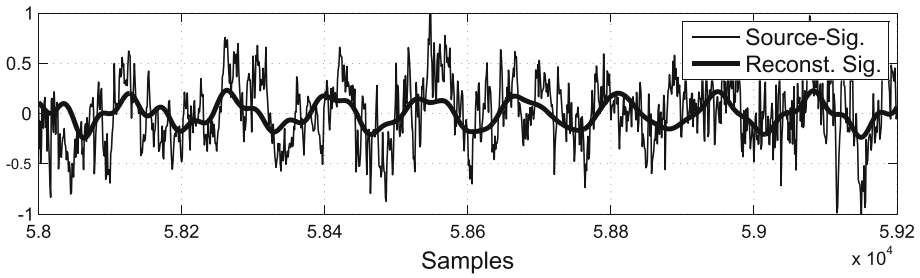

Fig. 24 Reconstruction of the signal acquired at $x/w = 4$, $y/w = 1$, $z/h = 0.9$

time-frequency analysis of the hot-wire signals, three spectral components have been simultaneously detected by using the first eight POD modes. These components have been found to be practically uncorrelated and, thus, related to the dynamics of three different vorticity structures, i.e., the vortex shedding from the vertical edges of the prism, the oscillation of a couple of axial vortices detached over the model free-end, and the oscillation of a transversal shear layer bounding the recirculation region lying behind the model.

Acknowledgments The authors would like to thank G. Buresti and L. Carassale for their invaluable suggestions and their contribution to the paper writing. Thanks are also due to M. V. Salvetti and to L. M. Pii.

References

Bendat JS, Piersol AG (1986) Random data: analysis and measurement procedures, 2nd edn. Wiley, New York

Broomhead D, King G (1986) Extracting qualitative dynamics from experimental data. Phys D 20:217–236

Buffoni M, Camarri S, Iollo A, Salvetti MV (2006) Low-dimensional modelling of a confined three-dimensional wake flow. J Fluid Mech 569:141–150

Buresti G, Iungo GV (2010) Experimental investigation on the connection between flow fluctuations and vorticity dynamics in the near wake of a triangular prism placed vertically on a plane. J Wind Eng Ind Aerodyn 98:253–262

Buresti G, Lombardi G, Bellazzini J (2004) On the analysis of fluctuating velocity signals through methods based on the wavelet and Hilbert transforms. Chaos Solitons Fractals 20:149–158

Camarri S, Salvetti MV, Buresti G (2006) Large-eddy simulation of the flow around a triangular prism with moderate aspect-ratio. J Wind Eng Ind Aerodyn 94(5):309–322

Carmona R, Hwang WL, Torresani B (1998) Practical time-frequency analysis. Academic Press, San Diego

Flandrin P, Rilling G, Gonçalvès P (2004) Empirical mode decomposition as a filter-bank. IEEE Signal Process Lett 11:112–114

Huang NE, Shen Z, Long SR, Wu MC, Shih HH, Zheng Q, Yen N, Tung CC, Liu HH (1998) The empirical mode decomposition and the Hilbert spectrum for non-linear and non-stationary time series analysis. Proc R Soc Lond Ser A Math Phys Eng Sci 454(1971):903–995

Huang NE, Wu Z, Long SR, Arnold KC, Chen X, Blank K (2009) On instantaneous frequency. Adv Adapt Data Anal 1(2):177–229

Iungo GV, Skinner P, Buresti G (2009) Correction of wandering smoothing effects on static measurements of a wing-tip vortex. Exp Fluids 46(3):435–452

Lumley JL (1970) Stochastic tools in turbulence. Academic Press, New York

Olhede S, Walden AT (2004) The Hilbert spectrum via wavelet projections. Proc R Soc Lond A 460:955–975

Pastur LR, Lusseyran F, Faure TM, Fraigneau Y, Pethieu R, Debesse P (2008) Quantifying the nonlinear mode competition in the flow over an open cavity at medium Reynolds number. Exp Fluids 44:597–608

Sirovich L (1987) Turbulence and the dynamics of coherent structures. Part I–III. Q Appl Math 45:561–590

Sreenivasan KR (1985) On the finite-scale intermittency of turbulence. J Fluid Mech 151:81–103

Vautard R, Yiou P, Ghil M (1992) Singular-spectrum analysis: a toolkit for short, noisy chaotic signals. Phys D 58:95–126